NeoBiota 84: 319–347 (2023)
doi: 10.3897/neobiota.84.90549
https://neobiota.pensoft.net

RESEARCH ARTICLE

A peer-reviewed open-access journal
NeoBiota
Advancing research on alien species and biological invasions

Conditions of emergence of the Sooty Bark Disease and aerobiology of *Cryptostroma corticale* in Europe

Elodie Muller[1,2*], Miloň Dvořák[3*], Benoit Marçais[1], Elsa Caeiro[4,5], Bernard Clot[6], Marie-Laure Desprez-Loustau[7], Björn Gedda[8], Karl Lundén[9], Duccio Migliorini[10,11], Gilles Oliver[12], Ana Paula Ramos[13], Daniel Rigling[14], Ondřej Rybníček[15], Alberto Santini[10], Salome Schneider[14], Jan Stenlid[9], Emma Tedeschini[16], Jaime Aguayo[2], Mireia Gomez-Gallego[1]

1 *Université de Lorraine, INRAE, IAM, Nancy 54000, France* **2** *ANSES Laboratoire de la Santé des Végétaux, Unité de Mycologie, USC INRAE 1480, Malzéville 54220, France* **3** *Department of Forest Protection and Wildlife Management, Mendel University in Brno, Brno 61300, Czech Republic* **4** *Sociedade Portuguesa de Alergologia e Imunologia Clínica - SPAIC, Lisbon, Portuga* **5** *Mediterranean Institute for Agriculture, Environment and Development - MED, Institute for Advanced Studies and Research, Universidade de Évora, Évora, Portuga* **6** *Federal Office of Meteorology and Climatology MeteoSwiss, Payerne 1530, Switzerland* **7** *University of Bordeaux, INRAE, BIOGECO, F- 33610 Cestas, France* **8** *Department of Environmental Research and Monitoring, Swedish Museum of Natural History, Stockholm 11418, Sweden* **9** *Department of Forest Mycology and Plant Pathology, Swedish University of Agricultural Sciences, Uppsala 75007, Sweden* **10** *National Research Council, Institute for Sustainable Plant Protection, 50019 Sesto fiorentino, Italy* **11** *School of Biological Sciences, University of Western Australia, Perth 6009, Australia* **12** *Réseau National de Surveillance Aérobiologique, Brussieu 69690, France* **13** *LEAF–Linking Landscape, Environment, Agriculture and Food, Instituto Superior de Agronomia, Universidade de Lisboa, 1349-017 Lisbon, Portugal* **14** *Research Unit Forest Health and Biotic Interactions, Swiss Federal Research Institute WSL, Birmensdorf 8903, Switzerland* **15** *Paediatric Department, University Hospital Brno and Medical Faculty, Masaryk University, Brno 62500, Czech Republic* **16** *Department of Agriculture Food and Environment Science, University of Perugia, Perugia 06121, Italy*

Corresponding author: Mireia Gomez-Gallego (mireia.gomez-gallego@inrae.fr)

Academic editor: Christelle Robinet | Received 19 July 2022 | Accepted 10 March 2023 | Published 18 May 2023

Citation: Muller E, Dvořák M, Marçais B, Caeiro E, Clot B, Desprez-Loustau M-L, Gedda B, Lundén K, Migliorini D, Oliver G, Ramos AP, Rigling D, Rybníček O, Santini A, Schneider S, Stenlid J, Tedeschini E, Aguayo J, Gomez-Gallego M (2023) Conditions of emergence of the Sooty Bark Disease and aerobiology of *Cryptostroma corticale* in Europe. In: Jactel H, Orazio C, Robinet C, Douma JC, Santini A, Battisti A, Branco M, Seehausen L, Kenis M (Eds) Conceptual and technical innovations to better manage invasions of alien pests and pathogens in forests. NeoBiota 84: 319–347. https://doi.org/10.3897/neobiota.84.90549

* These authors contributed equally to this work.

Copyright *Elodie Muller et al.* This is an open access article distributed under the terms of the Creative Commons Attribution License (CC BY 4.0), which permits unrestricted use, distribution, and reproduction in any medium, provided the original author and source are credited.

Abstract

The sooty bark disease (SBD) is an emerging disease affecting sycamore maple trees (*Acer pseudoplatanus*) in Europe. *Cryptostroma corticale*, the causal agent, putatively native to eastern North America, can be also pathogenic for humans causing pneumonitis. It was first detected in 1945 in Europe, with markedly increasing reports since 2000. Pathogen development appears to be linked to heat waves and drought episodes. Here, we analyse the conditions of the SBD emergence in Europe based on a three-decadal time-series data set. We also assess the suitability of aerobiological samples using a species-specific quantitative PCR assay to inform the epidemiology of *C. corticale*, through a regional study in France comparing two-year aerobiological and epidemiological data, and a continental study including 12 air samplers from six countries (Czechia, France, Italy, Portugal, Sweden and Switzerland).

We found that an accumulated water deficit in spring and summer lower than -132 mm correlates with SBD outbreaks. Our results suggest that *C. corticale* is an efficient airborne pathogen which can disperse its conidia as far as 310 km from the site of the closest disease outbreak. Aerobiology of *C. corticale* followed the SBD distribution in Europe. Pathogen detection was high in countries within the host native area and with longer disease presence, such as France, Switzerland and Czech Republic, and sporadic in Italy, where the pathogen was reported just once. The pathogen was absent in samples from Portugal and Sweden, where the disease has not been reported yet. We conclude that aerobiological surveillance can inform the spatial distribution of the SBD, and contribute to early detection in pathogen-free countries.

Keywords

Acer pseudoplatanus, aerobiology, airborne fungal spores, climate change, drought-induced forest disease, heat wave, invasive pathogen, maple bark disease, quantitative species-specific PCR

Introduction

Emerging infectious diseases threaten human health, agriculture and biodiversity (Jones et al. 2008). The occurrence of emerging diseases in forest ecosystems has exponentially increased over the last four decades in Europe (Santini et al. 2013), and the number of fungal plant diseases has shown a 13-fold worldwide increase in 15 years (Fisher et al. 2012). The most common drivers of new forest disease emergence are the introduction of exotic pathogens in new geographic areas and climate change (Ghelardini et al. 2016). Exotic pathogens have coevolved with hosts from their native range under particular environmental conditions and with particular associated microorganisms (Desprez-Loustau et al. 2007; Stenlid and Oliva 2016). The introduction of exotic pathogens to new geographic areas can potentially lead to severe disease outbreaks due to their encounter with naïve hosts, to the release of natural enemies, and to more favourable environmental conditions. Moreover, climate change can result in nonlinear range shifts of infectious forest diseases, as it can simultaneously affect the host's and pathogen's ecological niches (Dudney et al. 2021). This multifactorial nature of disease emergence may hinder proper epidemics' prediction and hence the establishment of appropriate disease management programmes.

Examples of forest diseases linked to climate extremes that are increasing in Europe are Diplodia tip blight in pine species (Brodde et al. 2019) and the Sooty Bark

Disease (SBD) in sycamore maple (*Acer pseudoplatanus*) trees (Bencheva 2014; Koukol et al. 2015). The SBD is caused by the ascomycete *Cryptostroma corticale*, putatively native to eastern North America (Ellis and Everhart 1889). In Europe, it was first reported in England in 1945 (Gregory and Waller 1951) and, in continental Europe, in France in 1951, followed by sporadic records in other European countries (Wilkins 1952; Cazaubon 2012). After 2000, SBD has been more frequently reported in Europe (Bencheva 2014; Cochard et al. 2015; Koukol et al. 2015; Oliveira Longa et al. 2016). The fungus has been described as an opportunistic pathogen, which particularly develops under high summer temperatures and drought stress (Abbey 1978; Ogris et al. 2021). It seems to remain in host tissues asymptomatically (Kelnarová et al. 2017) and to invade the cambium and the phloem of affected trees (Gregory and Waller 1951) when those extreme weather conditions occur. The infection can progress slowly for several years, but extensive tissue colonisation and damage have been reported one to two years after a very warm summer weather in England (Abbey 1978). The SBD is characterised, in its early stages, by generic symptoms such as wilt, branch dieback and epicormic shoots (Gregory and Waller 1951). But, in advanced stages, bark shedding exposing the fungal black stroma with a mass of spores is a typical symptom of SBD (Gregory and Waller 1951). According to the observations made by Gregory and Waller (1951) and Abbey (1978), the main mass of spores may be discharged after a heat wave or drought episode, but the SBD could develop at low intensity in the limb of the tree before becoming acute. However, the aetiology of the disease is not fully elucidated. The interest in studying SBD arises, on the one hand, from its increasing presence in Europe and its association with climate warming. On the other hand, the spores of *C. corticale* cause hypersensitivity pneumonitis in humans (Braun et al. 2021), currently called Maple Bark Stripper Lung (WHO 2022). This human disease was previously called Maple Bark Disease (MBD) and was first described in 1932 on woodmen, foresters and mill workers in eastern North America that were in contact with logs of *Acer* species with the presence of the fungus (Emanuel et al. 1962; Plate and Schneider 1965; Braun et al. 2021). The concern for a possible increasing risk of the disease in humans as a result of a greater presence of SBD in Europe, as the One Health approach anticipates (Destoumieux-Garzón et al. 2018), calls for the need to study the actual progress of the epidemic.

The SBD spread is likely to be limited by the occurrence of drought and heat wave episodes, that promote the infection process of the introduced pathogen itself. Monitoring SBD presence therefore requires good surveillance methods that are not dependent on the identification of symptoms in the host as those occur mainly after extreme weather and in the advanced stages of the disease. The conidia of *C. corticale* have been speculated to disperse by wind (Gregory and Waller 1951). Thus, aerobiology, which studies biological particles in the air, seems an appropriate approach to monitor the disease epidemic and to detect the disease in new areas before the appearance of symptoms on local sycamore maple trees. Particularly, we aim at testing the suitability of aerobiological samples from the pollen-monitoring network existing in Europe to assess *C. corticale* presence, as they proved adequate for other forest pathogens (Aguayo et al. 2020).

The objectives of the present study are therefore: (1) to develop a real-time PCR assay for the detection of *C. corticale* spores in aerobiological samples; (2) to analyse the conditions of emergence of the SBD in Europe through the study of time-series data of SBD occurrence and climatic data from France and Switzerland; (3) to analyse the dispersion of the pathogen *C. corticale* by wind at a regional scale, and (4) to study its presence on aerobiological samples at a continental scale.

Materials and methods

Study of pathogen emergence in France and Switzerland

Time series data collection

To analyse the emergence of SBD and its potential link to climate, we analysed complete time-series data of disease occurrence in France and Switzerland during the last three decades, from 1990 to 2021 and modelled this occurrence as a function of different climatic variables. The French disease records during these three decades were obtained from the database of the French Forest Health Department (DSF, French acronym). This database contains annual records of forest health problems observed in France by a network of foresters trained for the diagnosis of abiotic, entomological or pathological damages. The Swiss data were obtained from the forest protection reports generated by the Swiss Federal Institute for Forest, Snow and Landscape Research (WSL) (Queloz et al. 2020). The records in this database are based on the specific symptoms of the disease and diagnostic in the respective laboratories when symptoms are not conclusive. To account for potential sampling bias in our database (i.e. different monitoring intensities across time and regions), we standardised our data following a procedure commonly-used in medical epidemiology (Lawson 2001), that has also been applied in forest pathology (Fabre et al. 2012). Briefly, we computed a record rate $RR_{ij} = NSBD_{ij}/NRef_{ij}$ where $NSBD_{ij}$ and $NRef_{ij}$ are, respectively, the number of SBD cases and the number of other reported health problems concerning sycamore maple other than SBD, for year i and country j. The $NSBD_{ij}$ is used here as a proxy for both the observation pressure and the density of the host which cannot be separated in the dataset. This report rate (RR_{ij}) was then standardised by dividing by the report rate over the entire data set, i.e. including all years (Eq. 1).

$$SRR_{ij} = \frac{NSBD_{ij}}{NRef_{ij}} \cdot \frac{NRef}{NSBD} \qquad \text{Eq. 1}$$

where *NSBD* and *NRef* are, respectively, the total number of SBD and reference cases for the entire data set. Thus, a value of X for SRR_{ij} means that the report rate is X times the average report rate. Therefore, we assumed that a SRR_{ij} higher than 1 was

an outbreak of the disease, as the reported number of cases exceeds the the basal level of the disease (considered to be the global average of our database, i.e. *NSBD*/*NRef*). The distribution of the SBD records in France and Switzerland are shown in Suppl. material 1.

The climatic data were obtained from Météo-France (SAFRAN database) computed on a daily basis on an 8-km resolution grid throughout France and Switzerland (except for the Tessin region, where these data were not available) (Suppl. material 1). We selected all points of the climate grid close to each SBD record made in the 1989–2021 period. We computed eight variables, related to high summer temperature and drought (Ogris et al. 2021) and to limiting winter conditions, to be used as predictors of the SBD occurrence: the average daily maximal temperature in summer (July-August, $T_{Xsummer}$), in spring (April-June, $T_{Xspring}$) and in the vegetative season (April-August, T_{Xveg}), the water balance calculated as the sum of the daily difference between rainfall (P) and Penman-Monteith evapotranspiration (ETP) in summer (July-August, $P\text{-}ETP_{summer}$), in spring (April-June, $P\text{-}ETP_{spring}$), in the vegetative season (April-August, $P\text{-}ETP_{veg}$), the number of days in the year where the temperature exceeds 25 °C (*n25*) and the average daily minimum temperature in winter (January-March, $T_{Nwinter}$). We chose the threshold of 25 °C, as it has been reported as the optimal growth temperature of *Cryptostroma corticale* (Ogris et al. 2021). The eight variables were computed for one, two and three years preceding each disease record, which potentially contributed to or impeded disease development. We did not include the year when the disease was recorded, because disease records occurred throughout the year and not only after summer.

Aerobiological study: experimental design, sample collection and data sources

The samples used as starting material in our aerobiological study consisted of microscope slides with a ca. 48-mm portion of Melinex tape (corresponding to 24 h ± 2 h, depending on the sampling time) from Hirst-type volumetric air samplers used to monitor airborne pollen grains and fungal spores by the aerobiology networks of the involved European countries. The Hirst-type air samplers (Hirst 1952) are active vacuum-pumped suction traps with a rotating drum containing the Melinex tape covered by an adhesive solution which captures the particles present in the air (Fig. 1). Further details can be found in Lacey and West (2006) and in European Norm EN 16868:2019. The samplers of the network are placed on rooftops, at least 10–15 m high. We performed DNA extractions and qPCR targeting *C. corticale* (see following sections) to assess the detectability of *C. corticale* in aerobiological samples and to quantify the spores captured during a 24-h period.

We undertook two studies, at a regional and a continental scale, to evaluate the use of permanent aerobiological networks to assess *C. corticale* epidemiological surveillance. The regional study focused on French samplers, while the continental study covered locations in six European countries over a wide latitudinal and longitudinal range: Czechia, France, Italy, Portugal, Sweden and Switzerland.

Figure 1. 7-day volumetric air sampler (Burkard Manufacturing Co Ltd, Hertfordshire, UK) in Brno (Czechia) installed on the roof of the University hospital, 15 m above ground to ensure landscape-scale monitoring. Photo credit for Aneta Lukačevičová.

Regional study

We selected samplers to cover the SBD outbreak in north-eastern France in 2017 and 2018, following a two-year-spanned drought episode (from 2017 to 2018). We

selected four samplers located in Mulhouse (the main focus of the outbreak), and in three locations at different distances from the main focus (with less records of the disease): Bart, Besançon and Strasbourg (Table 1, Fig. 2). We selected four additional locations in the south of France, which were available for the year 2018, and had lower historical records of the disease (Angoulême, Aurillac, Avignon and Gap; Table 1, Fig. 2). To determine the optimal sampling period, we analysed the detectability of *C. corticale* in a temporal series of aerobiological samples from Mulhouse every three days from the 1st of May to the 30th of September of 2018. The highest frequency of spores was detected in May and June. Accordingly, the sampling period and intensity for the regional study were fixed in May-June with a three-day frequency, i.e. 10 samples per location and year.

In order to align the aerobiological data with the presence of the disease, we used the disease records from the DSF database (as described above). From 1989 to 2021, 1708 health reports were done on maples, of which 1351 were on

Table 1. Selected French air samplers for the regional study with different SBD incidence.

City	Code	GPS Coordinates	Year of the first record at < 50 km	Year of the first record at < 100 km	Year of the first record at < 180 km
Mulhouse	MUL	47.7524, 7.3591	2010	2010	1992
Bart	BAR	47.4856, 6.7694	no records	2010	1992
Besançon	BES	47.2324, 6.0231	no records	2006	1992
Strasbourg	STR	48.5833, 7.7500	no records	2010	2010
Angoûleme	ANG	45.6494, 0.1645	no records	2016	1991
Aurillac	AUR	44.9258, 2.4341	no records	no records	2014
Avignon	AVI	43.9203, 4.8021	no records	no records	2002
Gap	GAP	44.5575, 6.0761	no records	no records	2002

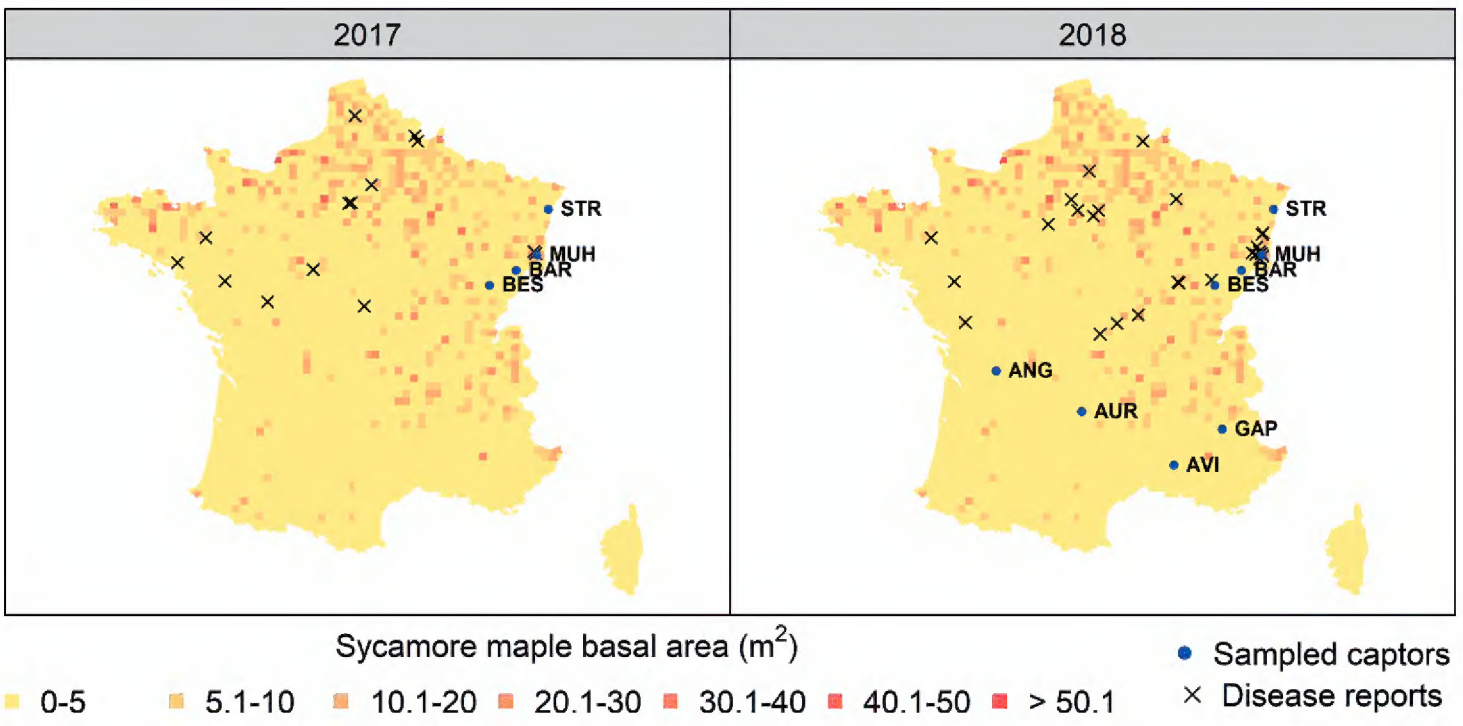

Figure 2. Selected air samplers, SBD records for years 2017 and 2018 considered for aerobiological sampling in 2017, and years 2018 and 2019 considered for 2018 sampling; and total sycamore maple basal area (m^2) in a 16×16 km grid.

A. pseudoplatanus and 172 corresponded to the SBD. We modelled the number of spores as a function of two variables: the distance to the disease and the maple basal area. We computed the distance to the closest disease record for each aerobiological sample (i.e. each captor) and year. We consider all the disease records taking place in both the year of the sampling and the following one, to capture the dispersion of the spores once the disease has been detected. Finally, we obtained host density data from the French National Forest Inventory (IFN, French acronym). We assigned to each sampler the sum of the total sycamore maple basal area in IFN plots in a radius of 50 km from each sampler, which is the reference area of influence of an aerobiological sampler (i.e. average distance at which the pollen is dispersed, Oteros et al. 2017), as a proxy for the host density. To test whether the radius at which we computed the maple basal area had an impact on its link to the number of spores, we tested a gradient of radius, from 40 to 130 km (by 10 km). Even though *C. corticale* can infect *Acer* spp. other than *A. pseudoplatanus*, such as *A. platanoides* and *A. campestre*, we only considered the latter in our study. Based on the French database, from all the SBD records from 1989 to 2021, *A. pseudoplatanus* is the main host (97.6% of cases).

Continental study

We selected a total of 12 air samplers across six European countries, spanning a large longitudinal and latitudinal range, in the axis north-south from Sweden to Portugal, and in the axis west-east from Portugal to Czechia (Table 2). The European samples were available every 12 days from the 1st of June to the 30th of September of 2018 (N = 10, per site), except for the French location of Gap, for which only June and July were available (N = 5).

Table 2. Locations of European air samplers for aerobiological samples analysed during the period from the 3rd of June to the 25th of September 2018, every 12 days (N = 10).

City	Code	GPS Coordinates	Country	Year first SBD record	Laboratory for DNA extraction
Brno	BRN	49.20374, 16.61800	Czechia	2005[1]	Mendel University (Czechia)
Gap	GAP	44.55750, 6.07610	France	1950[2]	INRAE Bordeaux (France)
Pontivy	PON	48.06670, -2.96830	France		INRAE Bordeaux (France)
Besançon	BES	47.23241, 6.02311	France		INRAE Bordeaux (France)
Bordeaux	BOR	44.80670, -0.58960	France		INRAE Bordeaux (France)
Bologna	BOL	44.49120, 11.36910	Italy	1952[3]	IPSP-CNR (Italy)
Perugia	PER	43.10091, 12.39593	Italy		IPSP-CNR (Italy)
Gävle	GÄV	60.67959, 17.14330	Sweden	Not reported	SLU (Sweden)
Visby	VIS	57.67336, 18.29269	Sweden		SLU (Sweden)
Lisbon	LIS	38.823718, -9.176685	Portugal	Not reported	SLU (Sweden)
Münsterlingen	MÜN	47.63040, 9.23679	Switzerland	1991[4]	WSL (Switzerland)
Payerne	PAY	46.81158, 6.94247	Switzerland		WSL (Switzerland)

[1] Koukol et al. 2015; [2] Cazaubon 2012; [3] Wilkins 1952; [4] Queloz et al. 2020.

Molecular detection of *C. corticale* in aerobiological samples

DNA extraction of aerobiological samples

Slides for the regional study were extracted in the laboratory of Forest Pathology at INRAE Nancy (France). For the continental study, the slides were extracted in different laboratories (Table 2), following the same procedure across studies and laboratories. Samples were processed according to the protocol by Aguayo et al. (2020). Briefly, mounted microscope slides were placed flat for 5–15 minutes on a constant heater set at 65 °C in order to unstick the glass cover slip. The sticky tape was recovered with laboratory forceps and cut into small pieces with sterile scissors. The tape pieces were then placed into tubes with screw caps containing one 3-mm sterile tungsten bead and 20 2-mm glass beads, and filled with 400 µl of AP1 buffer and 4 µl of RNase A (both from the DNeasy plant minikit Qiagen, Hilden, Germany). This mix was ground twice for 60 s (with a short cooling break) using a high-speed homogeniser, such as FastPrep 24 (MP Biomedicals) set at 6 m s^{-1} (INRAE Nancy, SLU Sweden and WSL Switzerland), Geno-Grinder (SPEX) with vertical shaking at 1500 rpm (INRAE Bordeaux), Mixer Mill MM400 (Retsch, Haan, Germany) set at 30Hz (Mendel University Czechia), and Mixer Mill 300 (Qiagen) (IPSP-CNR Italy). The genomic DNA from samples was then extracted with the Qiagen DNeasy plant minikit, following the manufacturers' specifications with a final DNA elution of 50 µl. Two types of negative controls were included in the extraction process. One control consisted of one vial left open while performing the slide preparation (one per day of extraction). Another one consisted of a negative control during the DNA extraction itself. The qPCR reactions (see next section) were performed at INRAE Nancy (France) for the regional study and at Mendel University (Czechia) for the continental study.

Development of a qPCR assay for *C. corticale*

The ITS region sequences with accurate identification were retrieved from GenBank for *C. corticale* and closely related species (*Biscogniauxia nummularia*, *B. mediterranea*, *B. latirima*, *B. philippinensis*, *Obolarina dryophila*, *Graphostroma platystoma*) to assure the specificity of the test. We also included, in the panel of species to be tested, species that are commonly found in *Acer* species, such as *Alternaria alternata*. Details of the included isolates are given in Suppl. material 2. We aligned the sequences using MUSCLE (Edgar 2004) implemented in Geneious V.R9 (https://www.geneious.com). The alignment was used to generate a series of couples of species-specific PCR primers and probes using Primer3 and Geneious. We evaluated melting temperatures and potential secondary structures in silico. Primer sequences were also checked for sequence homology with other DNA sequences by performing a BLAST search in GenBank. Further, we validated the specificity and inclusivity of the selected primers and probe by conventional PCR performed in a number of DNA extracts of *C. corticale* and non-target species (Suppl. material 2). The qPCR reactions were

performed with a QuantStudio 6 (Applied Biosystems, Carlsbad, USA) in 20 µl volumes containing 10 µl 1X Brilliant II QPCR Master Mix (Agilent Technologies), 0.3 µM of each primer, 0.1 µM probe, 0.01 Uracil DNA Glycosylase (UDG) U/µl, 30 nM reference dye, 2 µl volume of DNA template, and PCR-grade water (up to 20 µl total volume). Thermal cycling conditions consisted of a UDG activation phase at 37 °C for 10 min, polymerase activation at 95 °C for 10 min, followed by 40 cycles of 10 s at 95 °C and 45 s at 62 °C. The limit of detection (LOD) was achieved by qPCR amplifications with ten-fold dilutions of DNA extracted from *C. corticale* mycelium following the same protocol like for other samples in this study. Extracted DNA was quantified with NanoDrop ONE (Ozyme). Serial dilutions from 1 ng/µl to 1 fg/µl of DNA per sample were tested indicating the lowest concentration as the LOD yielding systematic Cq values.

C. corticale detection in aerobiological samples

Samples were run in triplicate in the regional study and in duplicate in the continental study, and both a negative (no template DNA) and a positive control (*C. corticale* mycelium DNA extract) were included in all series of reactions. Previous experience using spore traps has shown that qPCR Cq values can be below the detection limit of the assays, which means that the pathogen is present in the samples, but not at quantifiable concentrations (cf. Grosdidier et al. 2017; Aguayo et al. 2018). In case of three replicates, a sample was considered positive when at least two out of the three replicates yielded a cycle threshold value (with no upper limit, cf. Grosdidier et al. 2017). In two-replicate runs, if one of the two replicates was negative, another two-replicate reaction was performed. If either the same result was achieved or the two replicates were positive, the sample was considered positive. Otherwise, the sample was considered negative.

To quantify the spores on each aerobiological sample, we prepared 5-fold serial dilutions of a spore solution obtained by adding purified water on the surface of a sporulating culture of a French *C. corticale* isolate, LSVM1510. Spore concentration was determined using a haemocytometer. We performed DNA extractions from of each of the five spore solutions spanning from 1144 to 2 spores/µl. We ran qPCR for the five DNA extracts in triplicate to obtain a standard curve. As both the initial volume and the final elution volume of the DNA extraction was 50 µl, to obtain the number of spores corresponding to each Cq, we multiplied the initial spore concentration per 2 µl used in the qPCR reaction. We then fitted a linear model with cycle threshold (Cq) as a function of the logarithm of the number of spores ($P < 0.0001$; $R^2 = 0.95$; $Cq = 37.0–1.2 \log(\text{number of spores/µl})$). The same DNA extractions for spore quantification were used to perform two different standard curves at the Forest Pathology laboratory at INRAE Nancy (France) for the regional study and at the Mendel University (Czechia) for the continental study, where the respective qPCR assays of the samples were performed.

Data analysis

Pathogen emergence study

We have fitted Bayesian models to test the different hypotheses as follows. To analyse the effect of the climatic conditions on the emergence of the SBD, we modelled the *SRR* as a function of $T_{X,summer}$, $P\text{-}ETP_{summer}$, and $P\text{-}ETP_{veg}$ that were calculated for one, two and three previous years (see section of data sources). We ran individual models due to the high collinearity between temperature and water balance. We then chose the model with lower deviance (comparing the 95% confidence interval of the deviance). The *SRR* followed a Poisson distribution (Eq. 2). We included a binomial process (Eq. 3) to account for zeros that arise in addition to those modelled by the Poisson process (i.e. failure to detect the disease in the field). Therefore, the model distinguished two potentially different processes that determine the occurrence of SBD: (1) the occurrence of conducive weather conditions so that the pathogen can develop and cause a number of disease cases, as a Poisson process, and (2) the detectability of the disease in the field which may depend on other factors such as the presence of inoculum (arrival of the exotic pathogen), as a binomial process. We compared models with and without the binomial process and chose the one with the lowest Deviance Information Criterion (DIC). Following Eq. 1 for the standardisation of the SBD records, and isolating the $NSBD_{ij}$, which is our response variable, we included the fraction $\frac{NRef}{NRef_{ij} \cdot NSBD}$, as an offset term in the deterministic equation of the model (Eq. 4).

$$\text{number of cases of SBD} \sim \text{Poisson}\,(\lambda_k * d_k) \qquad \text{Eq. 2}$$

where k is the observation at a given sampler and date, λ_k is the number of spores, and d_k is the detectability of the disease, which follows a Bernoulli distribution (Eq. 3).

$$d_k \sim \text{Bernoulli}\,(p) \qquad \text{Eq. 3}$$

$$\log(\lambda_k) = alpha_k + beta * predictor_i + \log\left(\frac{NRef}{NRef_{ij} \cdot NSBD}\right) \qquad \text{Eq. 4}$$

where *alpha* is the intercept which varies for each year, *j* is the year, *beta* is the parameter estimate for the *predictor*, which can be any of the variables (cf. to the section 'Time series data collection').

Aerobiological study

We modelled the number of spores detected per week as a function of the distance to the closer disease report (model distance) and as a function of the total sycamore maple basal area in a radius of 50 km from the sampler (model host). We did not include the distance to the disease report and the total sycamore maple basal area as predictors in the

same model because their high collinearity prevented model convergence. The two models followed a Poisson distribution (Eq. 5), with lambda varying for each observation following a Gamma distribution to deal with overdispersion (Eq. 6–8). We included a binomial process (Eq. 9) to account for zeros that arise in addition to those modelled by the Poisson process (i.e. sampler's failure to capture spores even if they are present in the air). Therefore, the model distinguished two potentially different processes that determine the number of *C. corticale* spores in the air: (1) the sampler's efficacy to capture spores, as a binomial process, and (2) the number of spores, as a Poisson process. Finally, we compared models with and without the binomial process and chose the one with the lowest Deviance Information Criterion (DIC). The number of samples per week (from 1 to 4) was added as an offset of the Poisson model (Eq. 10). In both cases, the best models were the ones including the binomial process, hence our data was zero-inflated.

$$\text{number of spores} \sim \text{Poisson}\ (\lambda_k * e_k) \quad \text{Eq. 5}$$

where k is the observation at a given sampler and date, λ_k is the number of spores, and e_k is the efficacy of the sampler (probability of capturing any spores), which follows a Bernoulli distribution (Eq. 6):

$$\lambda_k \sim \text{Gamma}\ (a_k, b_k) \quad \text{Eq. 6}$$

where a_k and b_i are the shape and rate of the Gamma distribution, which relate to the mean number of spores and to the standard deviation (sigma) as follows (Eq. 4–5):

$$a_k = spores_k \text{^}2 \ / \ sigma\text{^}2 \quad \text{Eq. 7}$$

$$b_k = spores_k \ / \ sigma\text{^}2 \quad \text{Eq. 8}$$

$$e_k \sim \text{Bernoulli}\ (p) \quad \text{Eq. 9}$$

$$\log(spores_k) = alpha + beta * predictor_k + \log(Nsam_k) \quad \text{Eq. 10}$$

where *alpha* is the intercept, *beta* is the parameter estimate for the *predictor*, which can be either the distance to the disease report (model distance) or the total sycamore maple basal area (model host), *Nsam* is the total number of samples analysed per week (offset term).

We modelled the probability of disease occurrence in a certain area of influence of the sampler (in a circumference of different radii, from 40 to 130 km of radius, by 10-km intervals) as a function of the number of detected spores. The two models followed a Bernoulli distribution (Eq. 10). The deterministic part of the model is shown in Eq. 11.

$$\text{Probability of disease occurrence in an area of 40 to 130 km radius} \sim \text{Bernoulli}\ (p_k) \quad \text{Eq. 11}$$

where k is the observation at a given sampler and date, and p_i is the presence-absence of the disease at the given distance (40 to 130 km) from the sampler.

$$\log(p_k) = alpha + beta * spores_k \quad \text{Eq. 12}$$

where *alpha* and *beta* are the parameters estimated by the model, and *spores* is the number of spores detected by the sampler.

To validate our models, we simulated data based on the likelihood of each model. We then compared the means, the coefficients of variation and the sums of squares of the residuals of the original dataset with each simulated dataset. The histogram of the differences for each statistic should be zero-centred, with the proportion of negative (or positive) differences being lower than 0.85 for the model to be accepted.

All Bayesian models were implemented using a Markov chain Monte Carlo (MCMC) sampler (JAGS, Just Another Gibbs Sampler; Plummer 2003) called from R (function jags.fit, package R2jags, Su and Yajima 2021). All models were fitted using three chains, 100 000 iterations with a 10 000 burn-in and noninformative priors. Chains were checked for convergence using the Gelman and Rubin diagnostic and the 95% credible intervals of the parameters and predictions were directly extracted from the estimated posterior distributions of the model (Rhat diagnostic). We simulated data for all the models following the corresponding distribution. We analysed the residuals of the simulated data and the predicted values of the model. The model was considered accurate if the residuals were zero-centred.

Results

qPCR assay for *C. corticale*

The selected primers and probe used in this study were ccITS2F (AGGTTGTGCTGTCCGGTG), reported in the study by Kelnarová et al. (2017), and the new reverse primer and probe developed here: SBD3R (AGCTCCTACCAACTACAGGGT) and SBD5P (FAM-ACCCTGTAGGAGGAGCTACCCTGTA-BHQ1), respectively. The LOD was fixed at 0.01 pg/µl (Cq 35.9 ± 0.2) in DNA extracts from mycelium samples (see Suppl. material 3). The detection of spores with our test ranged from 2 to 1144 spores/µl.

Pathogen emergence in France and Switzerland

The climatic variable best explaining the standardised SBD report rate was the water balance (*P-ETP*) in the vegetative season (April-August) of the year preceding the disease report (Table 3). Other models that yielded low deviance were the water balance in the summer of the year preceding disease, the mean number of days with temperature exceeding 25 °C of the two previous years of disease record, and the water balance in the spring of the year preceding disease (Table 3). We found that *SRR* was predicted to exceed 1 when at least 33 days per year (95% CI 29, 36) had a temperature higher than 25 °C during the two years preceding disease. The distribution of the residuals of the best model (water balance in the vegetative season) can be found in Suppl. material 4.

Table 3. Coefficient estimates for each climatic variable and their 95% credible intervals in brackets for models predicting the standardised SBD case rate per year. Estimates are generated from the posterior distributions of the variables in the Poisson model (Eq. 11). Each climatic variable is calculated for either the previous year (n-1), two (n-1 to n-2) or three (n-1 to n-3) previous years. Rhat is the potential scale reduction factor and indicates whether the model has converged. Successful convergence is reached when Rhat values are < 1.1. T_X: average daily maximal temperature; T_N: average daily minimal temperature; *P-ETP*: Water balance as the sum of the daily difference between rainfall and Penman-Monteith evapotranspiration; n25: number of days per year where the temperature exceeds 25 °C; summer: July-August; spring: April-June; winter: January-March; veg: April-August.

Variable	Years	Coefficient estimate [95% CI]	Rhat	Deviance [95% CI]
$T_{X,summer}$	n-1	1.19 [0.74, 1.68]	1.0012	209.1 [193.2, 228.3]
$T_{X,spring}$		1.21 [0.77, 1.70]	1.0009	199.1 [183.7, 217.9]
T_{Xveg}		1.15 [0.78, 1.53]	1.0009	201.0 [185.9, 218.8]
$T_{Nwinter}$		0.66 [0.43, 0.89]	1.0009	199.0 [183.9, 217.1]
$P\text{-}ETP_{summer}$		-1.08 [-1.38, -0.78]	1.0009	188.3 [172.7, 207.5]
$\boldsymbol{P\text{-}ETP_{veg}}$		**-1.15 [-1.46, -0.85]**	**1.0009**	**183.6 [169.3, 200.5]**
$P\text{-}ETP_{spring}$		-1.35 [-1.85, -0.89]	1.0009	192.2 [178.1, 209.5]
n25		1.16 [0.78, 1.58]	1.0009	208.0 [193.2, 227.1]
$T_{X,summer}$	n-1 to n-2	1.37 [0.86, 1.98]	1.0009	197.9 [182.0, 217.9]
$T_{X,spring}$		1.23 [0.77, 1.71]	1.0013	203.0 [187.8, 221.5]
T_{Xveg}		1.25 [0.87, 1.66]	1.0009	196.1 [181.0, 214.3]
$T_{Nwinter}$		0.64 [0.41, 0.87]	1.0009	202.8 [187.9, 221.0]
$P\text{-}ETP_{summer}$		-1.08 [-1.50, -0.70]	1.0009	200.0 [185.8, 218.1]
$P\text{-}ETP_{veg}$		-1.07 [-1.50, -0.68]	1.0001	208.6 [193.7, 227.1]
$P\text{-}ETP_{spring}$		-0.74 [-1.26, -0.27]	1.0009	227.0 [212.3, 244.8]
n25		1.40 [0.94, 1.90]	1.0010	191.0 [175.5, 210.7]
$T_{X,summer}$	n-1 to n-3	0.83 [0.32, 1.43]	1.0009	222.2 [206.5, 241.2]
$T_{X,spring}$		1.21 [0.78, 1.65]	1.0009	201.0 [186.6, 218.9]
T_{Xveg}		1.09 [0.71, 1.49]	1.0009	205.8 [191.6, 222.8]
$T_{Nwinter}$		0.72 [0.49, 0.95]	1.0009	201.5 [187.1, 218.6]
$P\text{-}ETP_{summer}$		-0.61 [-1.10, -0.16]	1.0009	227.7 [212.5, 246.5]
$P\text{-}ETP_{veg}$		-0.50 [-0.85, -0.16]	1.0009	225.9 [211.7, 244.6]
$P\text{-}ETP_{spring}$		-0.42 [-0.80, -0.06]	1.0009	227.4 [214.2, 244.9]
n25		1.16 [0.57, 1.88]	1.0009	211.3 [194.8, 231.4]

The number of SBD cases increased exponentially with more negative water balance (Fig. 3a). On average, the model predicted a standardised SBD report rate higher than 1 (i.e. SBD occurrence higher than average) for total water balance in spring and summer lower than -132 mm (95% CI -170, -93, Fig. 3a), which qualifies a mild drought (extreme drought events taking place around -300 and -400 mm of *P-ETP*, Candel-Pérez et al. 2012). The number of SBD cases in France was on average higher than in Switzerland, corresponding to more negative accumulated water deficit during the vegetative season (Fig. 3b). SBD peaks in France paralleled those in Switzerland, with a marked increase from 2018 to 2021. Even though drought peaks in both countries did not appear to increase in magnitude across the years, they did

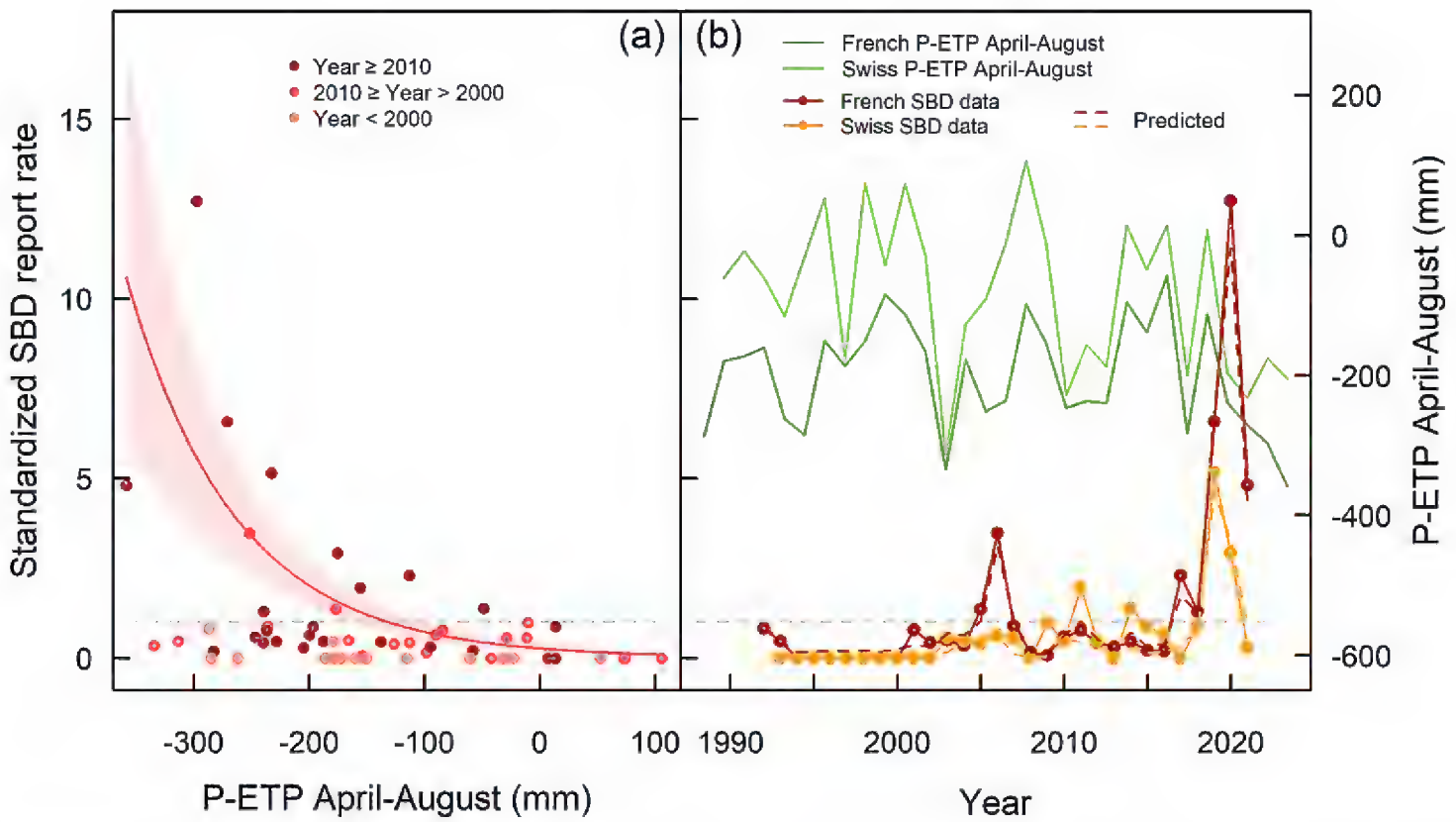

Figure 3. Model prediction of standardised SBD report rate as a function of water balance (measured as *P-ETP*) of the vegetative season (April-August) of the year previous to the disease report (**a**). Evolution of standardised SBD reports from 1990 to 2021 in France and Switzerland (**b**), and model predictions (Eq. 2). A dotted grey line indicates a standardised record rate that equals 1, above which the number of cases of the SBD is higher than average, and hence considered an outbreak of the disease.

tend to be more frequent after 2005 (Fig. 3b). No annual point earlier than 2005 exceeded the average report rate (*SRR* above 1, Fig. 3b). According to our model, the probability of disease absence not being linked to the water balance of the vegetative season (i.e. Bernoulli process, Eq. 3) was 0.05 (95% CI 0, 0.19). This zero-inflation, not explained by the water deficit, was mostly observed during the first decade of the time-series (Fig. 3).

Regional study

The number of spores detected per week was more abundant in samplers closer to disease reports (Fig. 4a). However, the magnitude of the increase was not large, and the coefficient estimate for the variable distance was not significant (i.e. the 95% CI contained the 0; Table 4). Our model predicted a detection of 27 spores per week (two sampling days per week) (95% CI 16, 40) at 10 km from the closest disease report, while 10 spores (95% CI 2, 25) were detected at a distance of 300 km (Fig. 4a). An increasing number of spores were detected in areas with a higher sycamore maple density (Fig. 4b). Even in areas with no sycamore maple in a radius of 50 km, the aerobiological samples presented *C. corticale* DNA, up to 20 spores. The coefficient estimate for the total sycamore maple area was positive on average, but not significant

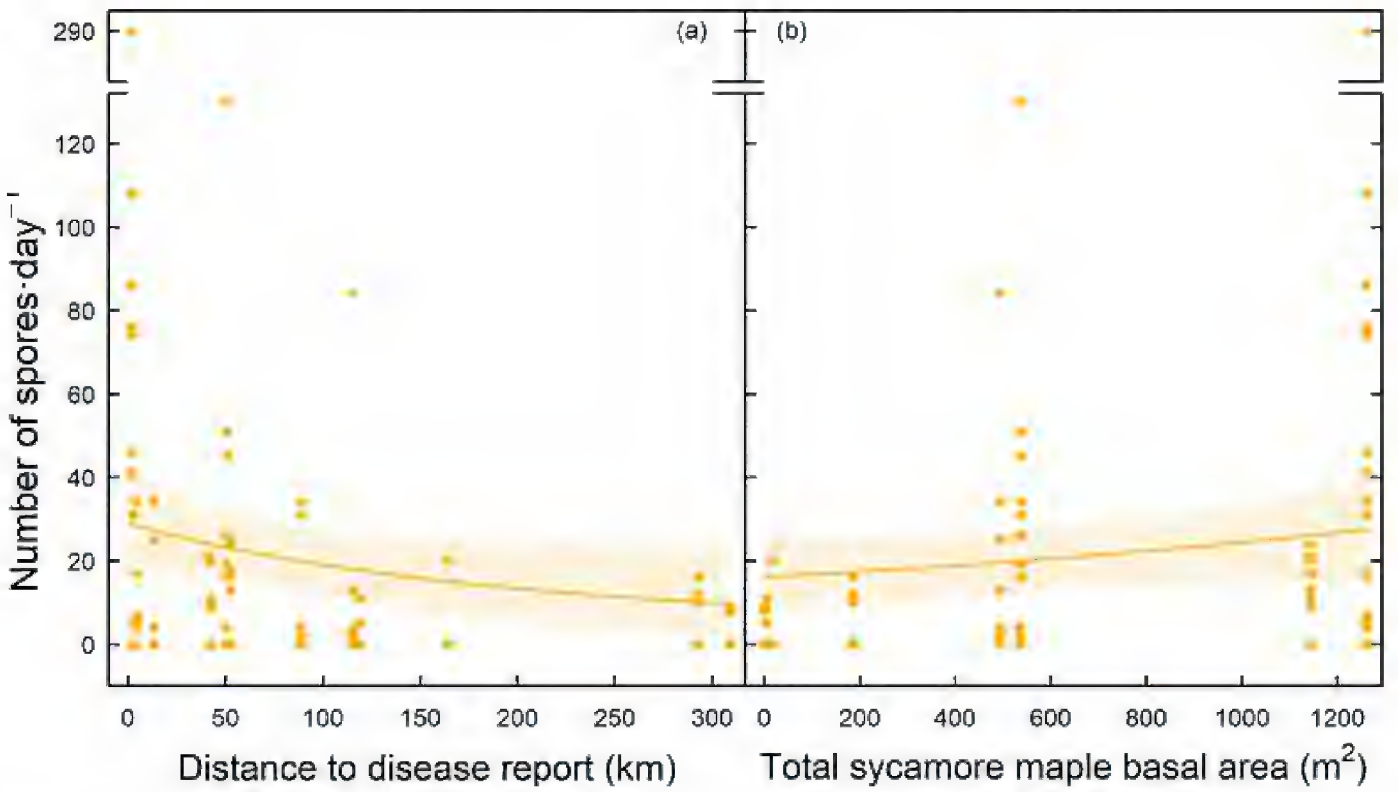

Figure 4. Number of spores per day as a function of the distance to the closest disease report (**a**), and as a function of the total maple basal area (m^2) in a radius of 50 km from the sampler (**b**).

(Table 4). The distribution of the residuals of the best models (distance to the closest disease report and total maple basal area in a 50-km radius from the sampler) can be found in Suppl. materials 4, 5, respectively. The other radius tested for the computation of the maple basal area showed the same deviance, hence no other radius value led to an estimation of maple basal area that better explained the presence of spores in the air (Suppl. material 7).

The two models (distance to the disease, and maple basal area) estimated a similar probability of spore capture (0.73 and 0.72, respectively, Bernoulli process in Eq. 8, Table 4). Therefore, 27% (or 28%) of the lack of spore detection (zero inflation) was due to a process other than the distance to the disease report (or the host density), and hence not explained by our deterministic model.

The probability of disease occurrence increased with the number of detected spores at a given distance (Fig. 5, Suppl. material 8). A 95% probability of disease in a radius of 60 km and 120 km corresponded to 41 and 127 spores detected, respectively. How-

Table 4. Parameter estimates and their 95% credible intervals in brackets for models describing spore detection as a function of distance to SBD reports and host density. Estimates are generated from the posterior distributions of the variables in the Poisson models (Eq. 6) with the variable response number of spores per week.

Response variable	**Detected spores per week**		
Parameter	**Intercept estimate**	**Coefficient estimate**	**Probability of spore capture**
Distance to disease report	2.64 [2.07, 3.07]	-0.41 [-0.97, 0.06]	0.73 [0.61, 0.85]
Total maple basal area	2.04 [1.41, 2.55]	0.04 [-0.01, 0.10]	0.72 [0.60, 0.85]

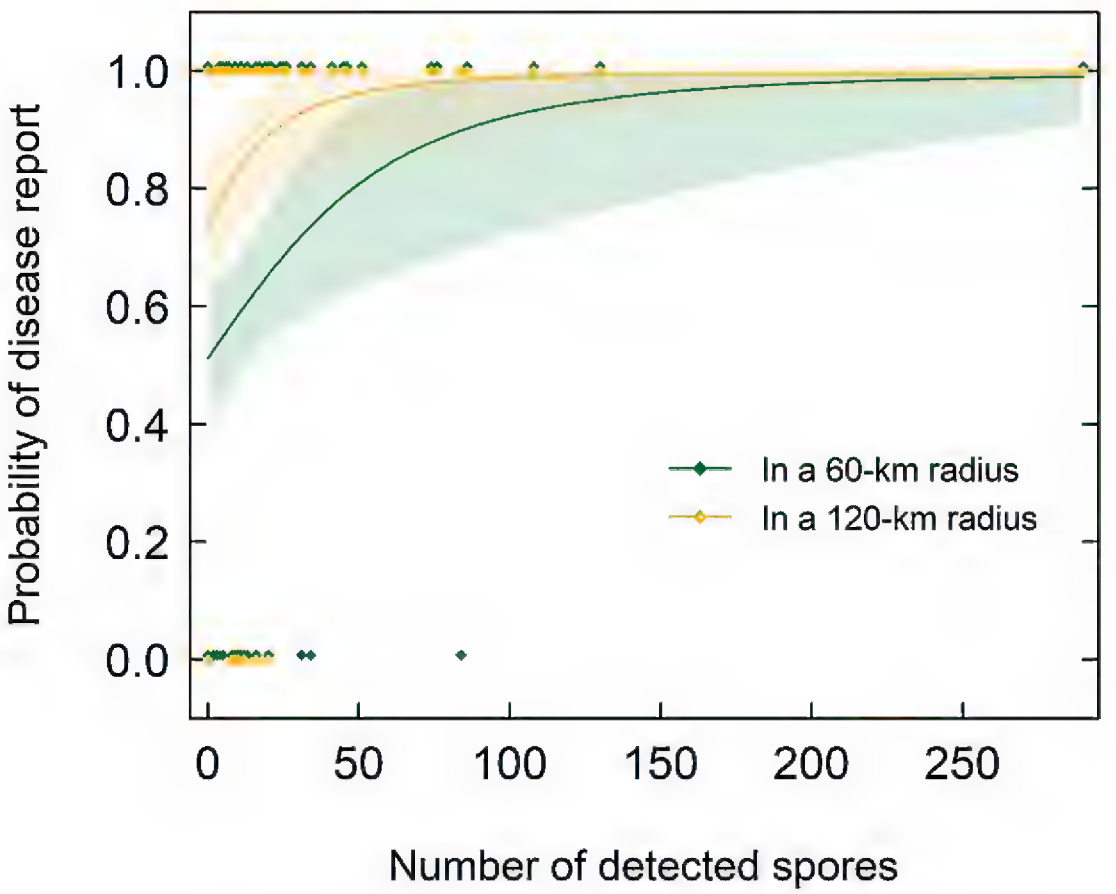

Figure 5. Probability of disease report in an area of 60-km and 120-km radius from the sampler as a function of the number of detected spores per day.

ever, the lack of spore detection did not correspond to the absence of disease reports. On the contrary, the disease could be detected in the field without being detected in aerobiological samples with two sampling days per week.

Continental study

The proportion of positive aerobiological samples based on the quantitative species-specific *C. corticale* PCR assay per year in Europe followed the reported presence of the disease in Europe (Fig. 6). Further, the regions that yielded more positive samples corresponded to those of the native range of sycamore maple, and hence with higher potential to maintain a sustained *C. corticale* population (samplers BES, PAY, MÜN and BRN, Fig. 6). Sweden and Portugal, the two countries where the disease had not been reported yet, did not present any positive samples (Figs 6, 7c, d). The highest proportions of positive samples were detected in France, Switzerland and Czechia (Figs 6, 7). Spores tended to be detected earlier in western than eastern locations. French samplers that produced positive samples, Bordeaux and Besançon, peaked spore detection in June and July, respectively (Fig. 7a). Payerne, in Switzerland, also presented a peak in July (Fig. 7b). Swiss location Münsterlingen and the Italian Bologna, presented higher *C. corticale* detection in August (Fig. 7b, e). Finally, the easternmost location in Czechia, Brno, peaked in September (Fig. 7f).

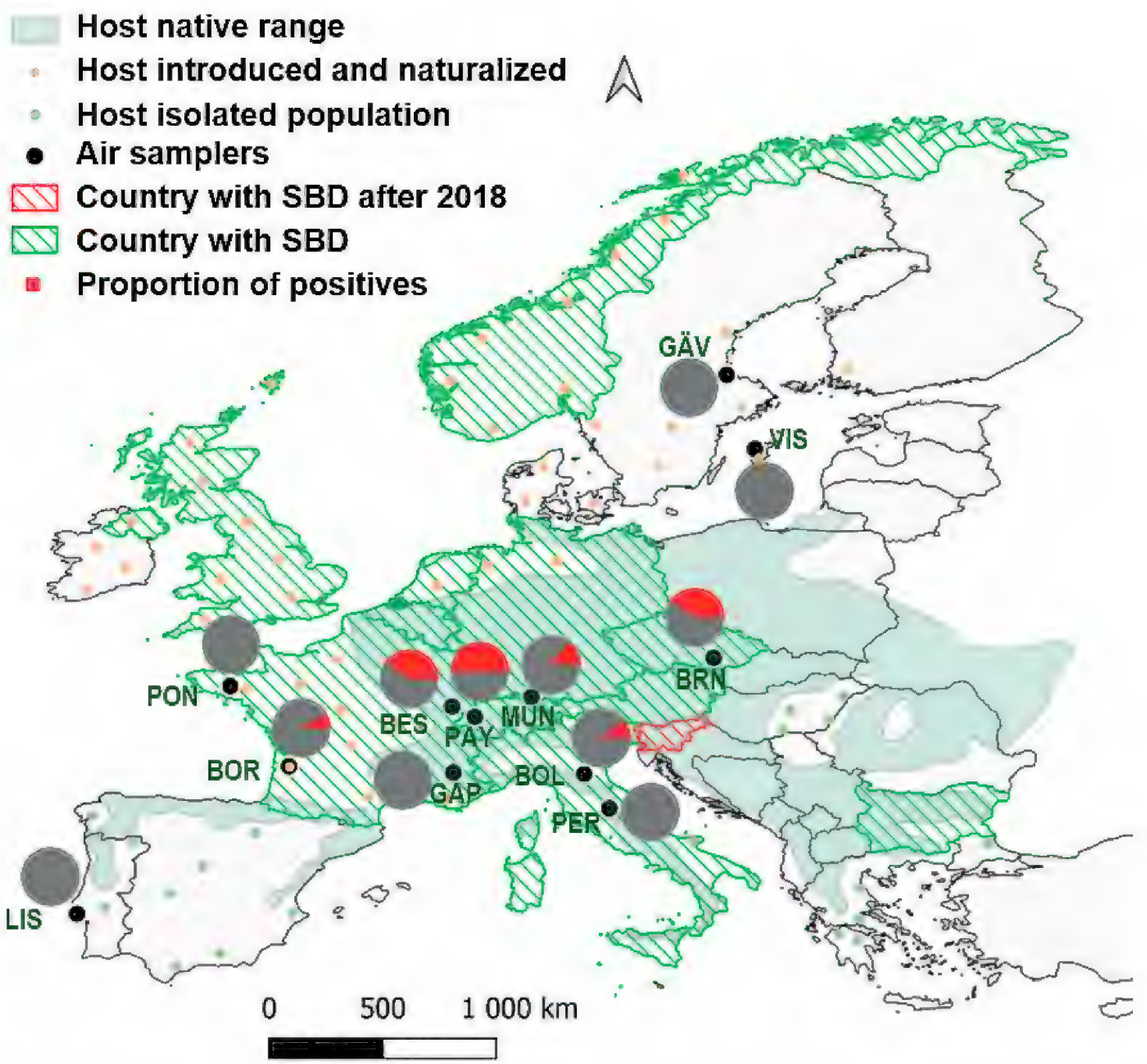

Figure 6. Proportion of aerobiological samples that tested positive from May to September of 2018 (n = 10, except for Gap where n = 5) in the different European samplers following the natural distribution of the host *Acer pseudoplatanus*.

Discussion

The present study aimed at analysing the emergence of SBD in Europe through the frequency of spore detection in aerobiological samples and time-series of disease records. Our results show that the SBD disease is at an exponentially increasing phase in France and Switzerland with an increase in the magnitude of the number of disease cases that peaks following a marked water deficit. Those episodic disease peaks do not show a deceleration, but they continue to increase in magnitude -the last peak is far higher than the precedent one (Fig. 3b)-, and they may continue to increase as drought events do. The spread of SBD has not occurred continuously, as in other invasive diseases like the ash dieback disease (Gross et al. 2014), due to the irregular, low-frequent nature of very hot and dry conditions needed for pathogen development (Ogris et al. 2021). Time-series data of SBD in France and Switzerland from 1990 to 2021 showed a series

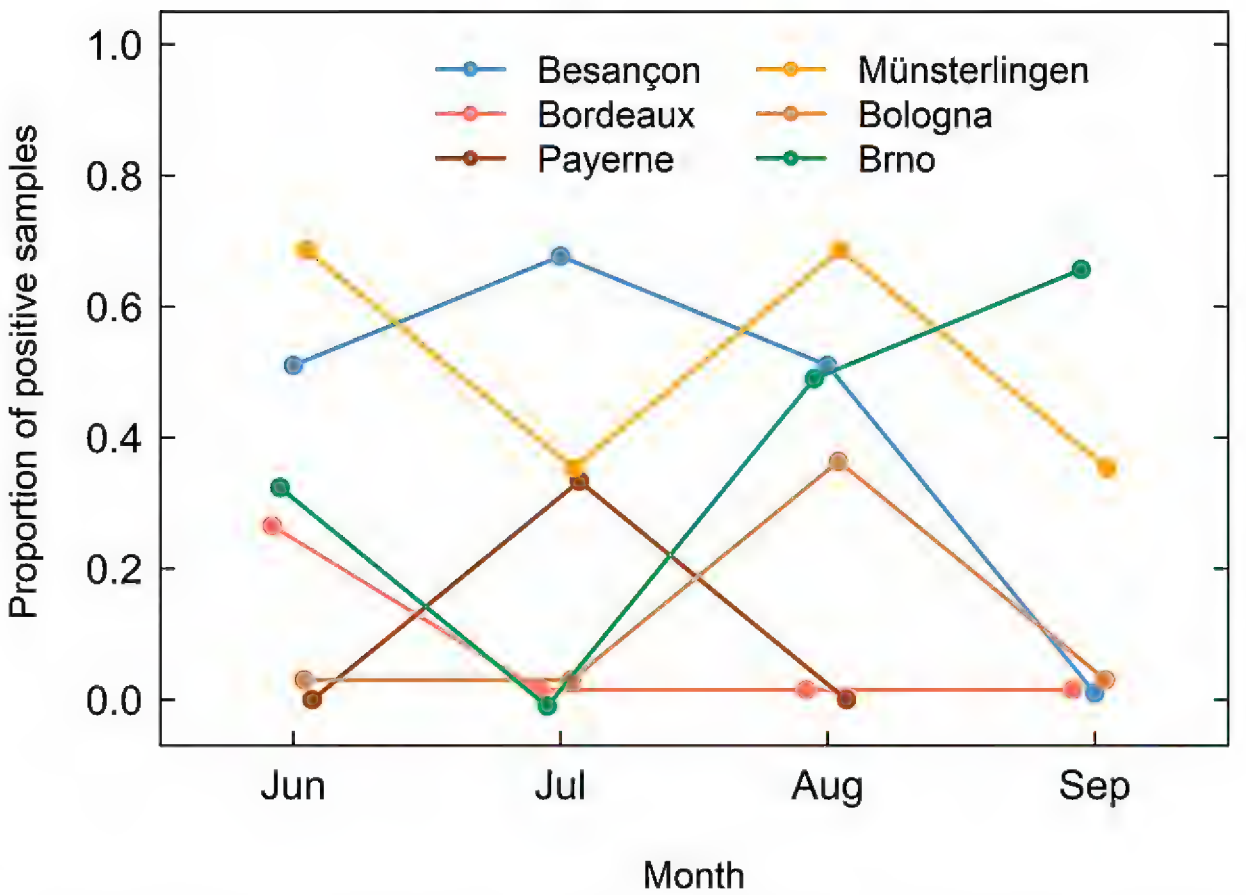

Figure 7. Phenology of spore emission of *Cryptostroma corticale* in the studied European countries showing the proportion of positive aerobiological samples per year. Jun: June; Jul: July; Aug: August; Sep: September.

of disease peaks coinciding with low spring and summer water balance and high temperatures. Our data show that drought favours pathogen development, as previously reported in experimental conditions (Ogris et al. 2021). However, as shown by our model using the number of days exceeding 25 °C, recorded disease outbreaks are also associated with high temperatures in the two previous years. Summer temperatures seem to control the internal spread of the fungus, with 25 °C as the optimal growth temperature in vitro (Abbey 1978; Ogris et al. 2021). We found this relationship in one of our best models. Outbreaks of the disease are associated with the occurrence of more than 33 days (95% CI 29, 36) with a temperature higher than 25 °C per year during the two years preceding the disease.

Temporal dynamic of the SBD

Disease peaks increased exponentially in magnitude with time. *C. corticale* is an invasive pathogen, reported for the first time in continental Europe in 1952, in France. In Switzerland, the first known report was in 1991. The highest peaks of the standardized number of disease records in 2020 in both countries suggest that the pathogen, after several outbreaks of the disease, might have colonized more forest plots, where the disease was eventually able to develop after conducive weather conditions. Two processes may have then taken place that explain the exponential increase in the last decades in France and Switzerland: (1) the dispersion and the establishment of the exotic

pathogen, and (2) an increasing frequency of low water balance and high temperatures which are conducive conditions for the SBD disease. The relative contribution of the two processes in the SBD emergence cannot be fully disentangled from our model. However, they are likely to have occurred additively, as the main dispersion events of the pathogen are highly dependent on drought conditions. Hence, the increased frequency of drought events and heat peaks might have led to higher dispersion rates. The estimation of the zero-inflation at 5% in our climate model suggests that the disease is mainly climate-driven (i.e. only 5% of disease absence is not explained by high water deficit in the vegetative season). Before 2005, there was no *SRR* higher than one, which implies an outbreak of the SBD (higher recording of SBD compared to average). The lack of SBD reports in early years may be due to the absence of inoculum (early phases of the invasive process) and the less frequent conducive conditions to the SBD. However, the lack of awareness of the disease by surveillance agents and hence little attention to symptoms in the field might have also resulted in fewer reports. Although the disease is detectable some months before sporulating lesions develop on the trunk (sooty appearance), those early symptoms are not specific to the SBD: wilting of leaves, presence of stool shoots and branch dieback (Gregory and Waller 1951). This means the disease is usually reported at its later stage. Further, the apparent similarity of dark brown stroma of *C. corticale* to black stroma of the common saprophytic fungus *Eutypa maura* (Fr.) Sacc. (Saccardo 1882) may be another reason for misidentification. Finally, the SBD is commonly found in urban environments, which are recognized to be an entry pathway for exotic pathogens (Tubby and Webber 2010; Paap et al. 2017), and hence expected to be, in proportion, more frequently found in urban areas than natural ecosystems in the early phases of pathogen invasion. Urban environments are, in addition, known to be heat islands with warmer and drier conditions than forests. These two reasons could thus also explain why early cases of the disease, being more frequent in urban areas, were poorly reflected in our time-series data which mostly included forested areas. In any case, the SBD occurrence rate in this study focuses on its emergence in forests, giving a temporal frame of the development of an invasive disease linked to climate extremes.

Aerobiology of *C. corticale*

The presence of *C. corticale* in aerobiological samples paralleled the presence of the disease SBD in Europe. At the continental level, monitoring of aerobiological samples shows a great potential as a large-scale epidemio-surveillance method for the SBD in Europe. Especially, early aerial detection of *C. corticale* in disease-free countries, such as Portugal and Sweden, could help implement special measures for SBD detection and eradication in the field. The advantage of aerobiological monitoring is that the aerobiological networks are already established and samples can be potentially obtained periodically. This method has already been proved for other forest pathogens such as *Hymenoscyphus fraxineus*, *Heterobasidion annosum* s.l., *Erysiphe alphitoides*, and *Melampsora larici-populina* (Aguayo et al. 2020). The anamorphic *C. corticale* produces

conidia emerging from conidiophores in the stroma formed between the inner and outer bark. Even though the release mechanism of conidia is still unknown, it has been suggested that, when the bark peels off, the spore mass of *C. corticale* is exposed and dispersed by wind (Gregory and Waller 1951; Bencheva 2014; Oliveira Longa et al. 2016). The number of spores has been reported to be approximately 30 to 179 million per square cm of black sooty layer (Abbey 1978). Our results suggest that the pathogen is effectively dispersed by wind. However, a few points should be considered if aerobiological surveillance is to be implemented for the SBD. First, our models estimated the detectability of the pathogen with a probability of 72%. This implies that in 28% of the cases, the pathogen's spores may be present in the air but either not captured by the air samplers, or not detected by qPCR. This explains why our model of the probability of disease presence predicts SBD occurrence with a probability of 50% in a 60-km-radius area even when no spores are detected by the samplers. Second, spore capture efficiency may be improved by increasing the spatial resolution of the selected air samplers or by considering the movement of air masses in the selection of locations. Third, the sampling period can impact the probability of detection. In the regional study, we sampled every three days in May and June. This period could be either intensified or prolonged during additional months. The results of the European sampling show that the sporulating period may be larger than we expected based on the Mulhouse captor we had analysed before this study (not shown). A whole-year period would also be informative, in future research, to evaluate fluctuations in spore release. Finally, our aerobiological data consists of two years in the regional study and one year in the continental study, in both cases with conducive climatic conditions. A longer time-series aerobiological data would allow for assessing whether inoculum production is detectable outside the period of outbreaks.

Distance tended to decrease the number of detected spores, but the magnitude of the effect was low and it was not significant (the confidence interval of parameter estimates contained 0). We detected *C. corticale* spores as far as 310 km from the closest disease report. This result suggests that the fungus can disperse long distances by wind. However, we cannot rule out the possibility of underreporting with unobserved SBD occurring closer to the samplers in urban settings. It is reasonable to assume that the main SBD foci in forests were registered in our database from 2017–2018 onwards, as the disease was well known at that time by the surveillance agents. But, outbreaks in parks or along roads may not have been as comprehensively included in our database. We did not sample locations at distances farther than 310 km. Therefore, we cannot establish the limit of aerial dispersal of the fungus. Other wind-borne pathogens have shorter dispersal distances, such as *H. fraxineus*, the causal agent of the ash dieback disease, whose spores can be detected up to 50–100 km from the disease front (Grosdidier et al. 2018). Our results support the idea that *C. corticale* is an efficiently dispersed pathogen. However, the high spore detection could have been remarkably favoured by the fact that the sampled years were affected by heat waves and the number of SBD cases was inherently high. Extended time-series aerobiological analyses are needed to further understand the epidemiology and dispersion pattern of the SBD.

The relatively abundant number of spores of *C. corticale* detected in the surveyed air samplers, placed in cities, reveals a potential risk to human health. The spores of *C. corticale* cause the MBD (Emanuel et al. 1962), currently called Maple Bark Stripper Lung (WHO 2022), a hypersensitivity pneumonitis, allergic asthma, flu-like infections and interstitial pneumonia (Braun et al. 2021). With drought predicted to increase in the Mediterranean basin and western and central Europe in the following decades (IPCC 2021), a further expansion and intensification of the SBD can be expected. Thus, the risks to human health and the environment are intertwined, as the One Health approach states. Surveillance of spore levels in the air is crucial to assess disease risk. We have presented here a suitable methodology, including the use of aerobiological samples to monitor the evolution of the SBD, that can also provide data to assess the potential risk of MBD to humans. Assessing SBD epidemiology at a continental scale implies access to harmonized databases of both pathogen occurrence and host density. We seemingly succeeded in our joint effort to homogenise molecular protocols to reduce the bias in molecular detection of *C. corticale* in aerobiological samples. However, there is a need to homogenise data from forest national inventories and disease reporting at the European level. That would allow models including larger geographical areas, which would provide a better understanding of disease dynamics.

Acknowledgements

This project has received funding from the European Union's Horizon 2020 Programme for Research & Innovation under grant agreement No 771271 (HOMED project, "HOlistic Management of Emergent forest pests and Diseases"), and from the research project SIAMOIS ("Smart and Innovative Monitoring Of airborne fungal Invaders by molecular methods") by the French laboratory of excellence LabEx ARBRE. We greatly appreciate the valuable assistance provided by Etienne Brejon-Lamartiniere, Laure Dubois, Julie Faivre d'Arcier, Manuela Branco Ferreira, Anaïs Gillet, Quirin Kupper, Aneta Lukačevičová, Miloslava Majerová, Sophie Strohecker, Fabrizio Cioldi. We thank the ARPAE Area Prevenzione Ambientale Metropolitana di Bologna, Italy, for providing part of the Italian samples analysed in this study. The mycology research unit of the ANSES Plant Health Laboratory is supported by a grant managed by the French National Research Agency as part of the French government's "Investing for the Future" (PIA) programme (ANR-11-LABX-0002-01, Laboratory of Excellence-ARBRE).

References

Abbey SD (1978) The morphology and physiology of *Cryptostroma corticale*. PHD Thesis. Loughborough University of Technology, Loughborough.

Aguayo J, Fourrier-Jeandel C, Husson C, Ioos R (2018) Assessment of passive traps combined with high-throughput sequencing to study airborne fungal communities. Applied and Environmental Microbiology 84(11): 1–17. https://doi.org/10.1128/AEM.02637-17

Aguayo J, Husson C, Chancerel E, Fabreguettes O, Chandelier A, Fourrier-Jeandel C, Dupuy N, Dutech C, Ioos R, Robin C, Thibaudon M, Marçais B, Desprez-Loustau ML (2020) Combining permanent aerobiological networks and molecular analyses for large-scale surveillance of forest fungal pathogens: A proof-of-concept. Plant Pathology 70(1): 181–194. https://doi.org/10.1111/ppa.13265

Bencheva S (2014) First report of *Cryptostroma corticale* (Ellis & Everh.) P.H. Greg. & S. Waller on *Acer platanoides* L. in Bulgaria. Silva Balcanica 15(2): 101–104.

Braun M, Klingelhöfer D, Groneberg DA (2021) Sooty bark disease of maples: The risk for hypersensitivity pneumonitis by fungal spores not only for woodman. Journal of Occupational Medicine and Toxicology 16(1): 1–7. https://doi.org/10.1186/s12995-021-00292-5

Brodde L, Camarero JJ, Sánchez-Miranda Á, Özdağ Ş, Castaño C, Luchi N, Adamson K, Oliva J, Drenkhan R, Migliorini D, Lehtijärvi A, Stenlid J (2019) Diplodia Tip Blight on Its Way to the North: Drivers of Disease Emergence in Northern Europe. Frontiers in Plant Science 9: e1818. https://doi.org/10.3389/fpls.2018.01818

Candel-Pérez D, Linares JC, Viñegla B, Lucas-borja ME (2012) Assessing climate – growth relationships under contrasting stands of co-occurring Iberian pines along an altitudinal gradient. Forest Ecology and Management 274: 48–57. https://doi.org/10.1016/j.foreco.2012.02.010

Cazaubon JL (2012) Le point sur: la maladie de la suie. Bulletin de Santé Du Végétal. Midi-Pyréenées. 4: 1–1.

Cochard B, Crovadore J, Bovigny PY, Chablais R, Lefort F (2015) First reports of *Cryptostroma corticale* causing sooty bark disease in *Acer* sp. in Canton Geneva, Switzerland. New Disease Reports 31(1): 1–8. https://doi.org/10.5197/j.2044-0588.2015.031.008

Desprez-Loustau ML, Robin C, Buée M, Courtecuisse R, Garbaye J, Suffert F, Sache I, Rizzo DM (2007) The fungal dimension of biological invasions. Trends in Ecology & Evolution 22(9): 472–480. https://doi.org/10.1016/j.tree.2007.04.005

Destoumieux-Garzón D, Mavingui P, Boetsch G, Boissier J, Darriet F, Duboz P, Fritsch C, Giraudoux P, Roux F, Le Morand S, Paillard C, Pontier D, Sueur C, Voituron Y (2018) The one health concept: 10 years old and a long road ahead. Frontiers in Veterinary Science 5: 1–13. https://doi.org/10.3389/fvets.2018.00014

Dudney J, Willing CE, Das AJ, Latimer AM, Nesmith JCB, Battles JJ (2021) Nonlinear shifts in infectious rust disease due to climate change. Nature Communications 12(1): e5102. https://doi.org/10.1038/s41467-021-25182-6

Ellis JB, Everhart BM (1889) New species of hyphomycetous fungi. Journal of Mycology 5(2): 68–72. https://doi.org/10.2307/3752309

Emanuel DA, Lawton BR, Wenzel FJ (1962) Maple-bark disease. Pneumonitis due to *Coniosporium corticale*. The New England Journal of Medicine 26(7): 333–337. https://doi.org/10.1056/NEJM196202152660704

Fabre B, Ioos R, Piou D, Marçais B (2012) Is the emergence of Dothistroma needle blight of pine in France caused by the cryptic species *Dothistroma pini*? Phytopathology 102(1): 47–54. https://doi.org/10.1094/PHYTO-02-11-0036

Fisher MC, Henk DA, Briggs CJ, Brownstein JS, Madoff LC, McCraw SL, Gurr SJ (2012) Emerging fungal threats to animal, plant and ecosystem health. Nature 484(7393): 186–194. https://doi.org/10.1038/nature10947

Ghelardini L, Pepori AL, Luchi N, Capretti P, Santini A (2016) Drivers of emerging fungal diseases of forest trees. Forest Ecology and Management 381: 235–246. https://doi.org/10.1016/j.foreco.2016.09.032

Gregory PH, Waller S (1951) *Cryptostroma corticale* and sooty bark disease of sycamore (*Acer pseudoplatanus*). Transactions of the British Mycological Society 34(4): 579–597, IN8–IN10. https://doi.org/10.1016/S0007-1536(51)80043-3

Grosdidier M, Aguayo J, Marc B, Ioos R (2017) Detection of plant pathogens using real-time PCR: How reliable are late Ct values? Plant Pathology 66(3): 359–367. https://doi.org/10.1111/ppa.12591

Grosdidier M, Ioos R, Husson C, Cael O, Scordia T, Marçais B (2018) Tracking the invasion: Dispersal of Hymenoscyphus fraxineus airborne inoculum at different scales. FEMS Microbiology Ecology 94(5): 1–11. https://doi.org/10.1093/femsec/fiy049

Gross A, Holdenrieder O, Pautasso M, Queloz V, Sieber TN (2014) *Hymenoscyphus pseudoalbidus*, the causal agent of European ash dieback. Molecular Plant Pathology 15(1): 5–21. https://doi.org/10.1111/mpp.12073

Hirst BYJM (1952) An automatic volumetric spore trap. Annals of Applied Biology 39(2): 257–265. https://doi.org/10.1111/j.1744-7348.1952.tb00904.x

IPCC (2021) Climate Change 2021: The Physical Science Basis. Contribution of Working Group I to the Sixth Assessment Report of the Intergovernmental Panel on Climate Change. In: Masson-Delmotte V, Zhai P, Pirani A, Connors SL, Péan C, Berger S, Caud N, Chen Y, Goldfarb L, Gomis MI, Huang M, Leitzell K, Lonnoy E, Matthews JBR, Maycock TK, Waterfield T, Yelekçi O, Yu R, Zhou B (Eds) Climate Change 2021: The Physical Science Basis. Cambridge University Press, Cambridge, United Kingdom and New York. https://doi.org/10.1017/9781009157896

Jones KE, Patel NG, Levy MA, Storeygard A, Balk D, Gittleman JL, Daszak P, IPCC (2021) Climate Change 2021: The Physical Science Basis. Contribution of Working Group I to the Sixth Assessment Report of the Intergovernmental Panel on Climate Change. In: Masson-Delmotte V, Zhai P, Pirani A, Connors SL, Péan C, Berger S, Caud N, Chen Y (Eds) Climate Change 2021: The Physical Science Basis. Cambridge University Press. [In Press]

Jones KE, Patel NG, Levy MA, Storeygard A, Balk D, Gittleman JL, Daszak P (2008) Global trends in emerging infectious diseases. Nature 451(7181): 990–993. https://doi.org/10.1038/nature06536

Kelnarová I, Černý K, Zahradník D, Koukol O (2017) Widespread latent infection of *Cryptostroma corticale* in asymptomatic *Acer pseudoplatanus* as a risk for urban plantations. Forest Pathology 47(4): 1–5. https://doi.org/10.1111/efp.12344

Koukol O, Kelnarová I, Černý K (2015) Recent observations of sooty bark disease of sycamore maple in Prague (Czech Republic) and the phylogenetic placement of *Cryptostroma corticale*. Forest Pathology 45(1): 21–27. https://doi.org/10.1111/efp.12129

Lacey ME, West JS (2006) The Air Spora – A Manual for Catching and Identifying Airborne Biological Particles. Springer-Verlag, Dordrecht, The Netherlands, 156 pp. https://doi.org/10.1007/978-0-387-30253-9

Lawson AB (2001) Statistical Methods in Spatial Epidemiology. Chichester, 277 pp.

Ogris N, Brglez A, Piškur B (2021) Drought Stress Can Induce the Pathogenicity of *Cryptostroma corticale*, the Causal Agent of Sooty Bark Disease of Sycamore Maple. Forests 12(3): e377. https://doi.org/10.3390/f12030377

Oliveira Longa CM, Vai N, Maresi G (2016) *Cryptostroma corticale* in the northern Apennines (Italy). Phytopathologia Mediterranea 55(1): 136–138. https://doi.org/10.14601/Phytopathol

Oteros J, Valencia RM, del Río S, Vega AM, García-Mozo H, Galán C, Gutiérrez P, Mandrioli P, Fernández-González D (2017) Concentric ring method for generating pollen maps. *Quercus* as case study. The Science of the Total Environment 576: 637–645. https://doi.org/10.1016/j.scitotenv.2016.10.121

Paap T, Burgess TI, Wingfield MJ (2017) Urban trees: Bridge-heads for forest pest invasions and sentinels for early detection. Biological Invasions 19(12): 3515–3526. https://doi.org/10.1007/s10530-017-1595-x

Plate H-P, Schneider R (1965) Ein Fall von asthmaartiger Allergie, verursacht durch den Pilz *Cryptostroma corticale*. Cryptostroma 1932: 100–101.

Plummer M (2003) JAGS: A program for analysis of Bayesian graphical models using Gibbs sampling. Proceedings of the 3rd International Workshop on Distributed Statistical Computing. R Foundation for Statistical Computing, Vienna. https://doi.org/10.1002/ana.1067

Queloz V, Forster B, Stroheker S, Odermatt O, Hölling D, Klesse S, Vögtli I, Dubach V (2020) Waldschutz Überblick 2019. In WSL Ber., 40 pp.

Saccardo PA (1882) Sylloge Fungorum. Abellini, 166 pp.

Santini A, Ghelardini L, De Pace C, Desprez-Loustau ML, Capretti P, Chandelier A, Cech T, Chira D, Diamandis S, Gaitniekis T, Hantula J, Holdenrieder O, Jankovsky L, Jung T, Jurc D, Kirisits T, Kunca A, Lygis V, Malecka M, Marçais B, Schmitz S, Schumacher J, Solheim H, Solla A, Szabo I, Tsopelas P, Vannini A, Vettraino AM, Webber J, Woodward S, Stenlid J (2013) Biogeographical patterns and determinants of invasion by forest pathogens in Europe. The New Phytologist 197(1): 238–250. https://doi.org/10.1111/j.1469-8137.2012.04364.x

Stenlid J, Oliva J (2016) Phenotypic interactions between tree hosts and invasive forest pathogens in the light of globalization and climate change. Philosophical Transactions of the Royal Society of London, Series B, Biological Sciences 371(1709): e20150455. https://doi.org/10.1098/rstb.2015.0455

Su YS, Yajima M (2021) R2jags: Using R to Run "JAGS". R package version 0.7-1. https://CRAN.R-project.org/package=R2jags

Tubby KV, Webber JF (2010) Pests and diseases threatening urban trees under a changing climate. Forestry 83(4): 451–459. https://doi.org/10.1093/forestry/cpq027

Wilkins VE (1952) Report of the technical working party. European Plant Protection Organization, Paris.

World Health Organisation (2022) CA70.6 Maple bark stripper lung. ICD-11 for Mortality and Morbidity Statistics.

Supplementary material 1

Records of SBD in France and Switzerland from 1990 to 2021 (red dots)

Authors: Elodie Muller, Miloň Dvořák, Benoit Marçais, Elsa Caeiro, Bernard Clot, Marie-Laure Desprez-Loustau, Björn Gedda, Karl Lunden, Duccio Migliorini, Gilles Oliver, Ana Paula Ramos, Daniel Rigling, Ondrej Rybnicek, Alberto Santini, Salome Schneider, Jan Stenlid, Emma Tedeschini, Jaime Aguayo, Mireia Gomez-Gallego

Data type: figure (word document)

Copyright notice: This dataset is made available under the Open Database License (http://opendatacommons.org/licenses/odbl/1.0/). The Open Database License (ODbL) is a license agreement intended to allow users to freely share, modify, and use this Dataset while maintaining this same freedom for others, provided that the original source and author(s) are credited.

Link: https://doi.org/10.3897/neobiota.84.90549.suppl1

Supplementary material 2

Isolates which DNA was extracted and used to confirm the specificity of the primers ccITS2F and SBD3R and probe SBD5P

Authors: Elodie Muller, Miloň Dvořák, Benoit Marçais, Elsa Caeiro, Bernard Clot, Marie-Laure Desprez-Loustau, Björn Gedda, Karl Lunden, Duccio Migliorini, Gilles Oliver, Ana Paula Ramos, Daniel Rigling, Ondrej Rybnicek, Alberto Santini, Salome Schneider, Jan Stenlid, Emma Tedeschini, Jaime Aguayo, Mireia Gomez-Gallego

Data type: table (word document)

Copyright notice: This dataset is made available under the Open Database License (http://opendatacommons.org/licenses/odbl/1.0/). The Open Database License (ODbL) is a license agreement intended to allow users to freely share, modify, and use this Dataset while maintaining this same freedom for others, provided that the original source and author(s) are credited.

Link: https://doi.org/10.3897/neobiota.84.90549.suppl2

Supplementary material 3

Standard curve and its correlation coefficient to determine the limit of detection for the real-time PCR assay in ten-folded DNA solutions of C. corticale mycelium (a) and total number of spores in the qPCR reaction (b)

Authors: Elodie Muller, Miloň Dvořák, Benoit Marçais, Elsa Caeiro, Bernard Clot, Marie-Laure Desprez-Loustau, Björn Gedda, Karl Lunden, Duccio Migliorini, Gilles Oliver, Ana Paula Ramos, Daniel Rigling, Ondrej Rybnicek, Alberto Santini, Salome Schneider, Jan Stenlid, Emma Tedeschini, Jaime Aguayo, Mireia Gomez-Gallego

Data type: figures (word document)

Copyright notice: This dataset is made available under the Open Database License (http://opendatacommons.org/licenses/odbl/1.0/). The Open Database License (ODbL) is a license agreement intended to allow users to freely share, modify, and use this Dataset while maintaining this same freedom for others, provided that the original source and author(s) are credited.

Link: https://doi.org/10.3897/neobiota.84.90549.suppl3

Supplementary material 4

Zero-centred histogram of the residuals between simulated data and predictions of the model with the water balance (P-ETP) in the vegetative season (April-August) of the year preceding disease report as a predictor of the standardized record rate of the SBD

Authors: Elodie Muller, Miloň Dvořák, Benoit Marçais, Elsa Caeiro, Bernard Clot, Marie-Laure Desprez-Loustau, Björn Gedda, Karl Lunden, Duccio Migliorini, Gilles Oliver, Ana Paula Ramos, Daniel Rigling, Ondrej Rybnicek, Alberto Santini, Salome Schneider, Jan Stenlid, Emma Tedeschini, Jaime Aguayo, Mireia Gomez-Gallego

Data type: figure (word document)

Copyright notice: This dataset is made available under the Open Database License (http://opendatacommons.org/licenses/odbl/1.0/). The Open Database License (ODbL) is a license agreement intended to allow users to freely share, modify, and use this Dataset while maintaining this same freedom for others, provided that the original source and author(s) are credited.

Link: https://doi.org/10.3897/neobiota.84.90549.suppl4

Supplementary material 5

Zero-centred histogram of the residuals between simulated data and predictions of the model with the distance to the closest disease report as a predictor of the number of *Cryptostroma corticale* spores detected in aerobiological samples

Authors: Elodie Muller, Miloň Dvořák, Benoit Marçais, Elsa Caeiro, Bernard Clot, Marie-Laure Desprez-Loustau, Björn Gedda, Karl Lunden, Duccio Migliorini, Gilles Oliver, Ana Paula Ramos, Daniel Rigling, Ondrej Rybnicek, Alberto Santini, Salome Schneider, Jan Stenlid, Emma Tedeschini, Jaime Aguayo, Mireia Gomez-Gallego

Data type: figure (word document)

Copyright notice: This dataset is made available under the Open Database License (http://opendatacommons.org/licenses/odbl/1.0/). The Open Database License (ODbL) is a license agreement intended to allow users to freely share, modify, and use this Dataset while maintaining this same freedom for others, provided that the original source and author(s) are credited.

Link: https://doi.org/10.3897/neobiota.84.90549.suppl5

Supplementary material 6

Zero-centred histogram of the residuals between simulated data and predictions of the model with the total sycamore maple basal area in a radius of 50 km from the sampler as a predictor of the number of *Cryptostroma corticale* spores detected in aerobiological samples

Authors: Elodie Muller, Miloň Dvořák, Benoit Marçais, Elsa Caeiro, Bernard Clot, Marie-Laure Desprez-Loustau, Björn Gedda, Karl Lunden, Duccio Migliorini, Gilles Oliver, Ana Paula Ramos, Daniel Rigling, Ondrej Rybnicek, Alberto Santini, Salome Schneider, Jan Stenlid, Emma Tedeschini, Jaime Aguayo, Mireia Gomez-Gallego

Data type: figure (word document)

Copyright notice: This dataset is made available under the Open Database License (http://opendatacommons.org/licenses/odbl/1.0/). The Open Database License (ODbL) is a license agreement intended to allow users to freely share, modify, and use this Dataset while maintaining this same freedom for others, provided that the original source and author(s) are credited.

Link: https://doi.org/10.3897/neobiota.84.90549.suppl6

Supplementary material 7

Coefficient estimate for each variable of maple basal area computed for different radius and their 95% credible intervals in brackets for models predicting the number of spores detected per week

Authors: Elodie Muller, Miloň Dvořák, Benoit Marçais, Elsa Caeiro, Bernard Clot, Marie-Laure Desprez-Loustau, Björn Gedda, Karl Lunden, Duccio Migliorini, Gilles Oliver, Ana Paula Ramos, Daniel Rigling, Ondrej Rybnicek, Alberto Santini, Salome Schneider, Jan Stenlid, Emma Tedeschini, Jaime Aguayo, Mireia Gomez-Gallego

Data type: table (word document)

Copyright notice: This dataset is made available under the Open Database License (http://opendatacommons.org/licenses/odbl/1.0/). The Open Database License (ODbL) is a license agreement intended to allow users to freely share, modify, and use this Dataset while maintaining this same freedom for others, provided that the original source and author(s) are credited.

Link: https://doi.org/10.3897/neobiota.84.90549.suppl7

Supplementary material 8

Probability of disease report in an area of 40-km to 130-km radius from the sampler as a function of the number of detected spores per day

Authors: Elodie Muller, Miloň Dvořák, Benoit Marçais, Elsa Caeiro, Bernard Clot, Marie-Laure Desprez-Loustau, Björn Gedda, Karl Lunden, Duccio Migliorini, Gilles Oliver, Ana Paula Ramos, Daniel Rigling, Ondrej Rybnicek, Alberto Santini, Salome Schneider, Jan Stenlid, Emma Tedeschini, Jaime Aguayo, Mireia Gomez-Gallego

Data type: figure (word document)

Copyright notice: This dataset is made available under the Open Database License (http://opendatacommons.org/licenses/odbl/1.0/). The Open Database License (ODbL) is a license agreement intended to allow users to freely share, modify, and use this Dataset while maintaining this same freedom for others, provided that the original source and author(s) are credited.

Link: https://doi.org/10.3897/neobiota.84.90549.suppl8